MARMARA UNIVERSITY
FACULTY OF ENGINEERING

COMPOSITE BASED AIR INTAKE PRODUCTION AND ANALYSIS

İREM BEYZA EKİCİ
MUSTAFA İLKER AKPINAR
ALPEREN SÖZER
ADEM CAN ALKAŞİ

GRADUATION PROJECT REPORT
Department of Mechanical Engineering

Supervisor
Prof. Dr. Emre ALPMAN

ISTANBUL, 2023

MARMARA UNIVERSITY
FACULTY OF ENGINEERING

COMPOSITE BASED AIR INTAKE PRODUCTION AND ANALYSIS

by

İREM BEYZA EKİCİ

MUSTAFA İLKER AKPINAR

ALPEREN SÖZER

ADEM CAN ALKAŞİ

June 22, 2023, Istanbul

SUBMITTED TO THE DEPARTMENT OF MECHANICAL ENGINEERING IN PARTIAL FULFILLMENT OF THE REQUIREMENTS FOR THE DEGREE

OF

BACHELOR OF SCIENCE

AT

MARMARA UNIVERSITY

Signature of Author(s) .....

Department of Mechanical Engineering

Certified By .....

Project Supervisor, Department of Mechanical Engineering

Accepted By .....

Head of the Department of Mechanical Engineering

ACKNOWLEDGEMENT

First of all, we would like to thank my supervisor Prof. Dr. Emre ALPMAN for the valuable guidance and advice on preparing this thesis and giving us moral. And we would like to thank to TAI and our Industry consultant Yahya ÖZ for their moral and material support.

June, 2023

İREM BEYZA EKİCİ
MUSTAFA İLKER AKPINAR
ALPEREN SÖZER
ADEM CAN ALKAŞİ

Content

Figures

Tables

Abstract

In this context, the project focuses on the analysis of variations in composite-based air inlet with different outlet pressures and Mach numbers, which can be used in our aircraft as supersonic and subsonic components, considering flight parameters. The design, miniature production, and analysis of an air inlet, which we believe will contribute to reducing our country's dependence on foreign sources, have been realized using open-source programs. The experiments and performance of the air inlet, which is the main topic of the project, have been subjects that have been studied for many years using various methods in different time periods. The value to be added here is to gain experience in the aviation sector and fluid dynamics by using open-source programs and applications, and to contribute to the country in the future by comparing theoretical calculations with actual experiments.

SYMBOLS

P : Pressure

n_t : inlet efficiency factor

Ma : Mach Number

P_t : Total Pressure

n_i : Inlet efficiency

K_f : Correction factor

D_{spill} : Spillage Drag

R_1 : Throat Radius

ABBREVIATIONS

PR : Pressure Recovery

MFR : Mass Flow Rate

CAD : Computer Aided Design

IPR : Inlet Pressure Recovery

AIP : Aerodynamic Interface Plane

CFD : Computational Fluid Dynamics

PDE : Partial Differential Equations

RAE : Royal Aircraft Establishment

SST : Shear Stress Transport

SA : Spalart–Allmaras

CFR : Carbon Fiber Reinforced

GCI : Grid Convergence Index

1. INTRODUCTION

Air breathing engines are engines that use the jet effect created by the exhaust gases, which are formed by the combustion of the air entering the air intake by mixing with the fuel, while leaving the engine. The performance of the jet engine depends on the correct design of the air intake. For this reason, it is extremely important to examine the flow in the air intakes correctly. The generally desired properties in air intakes can be listed as follows; To provide the required flow for the engine, to compress the incoming air effectively to minimize the total pressure loss, to have low drag coefficients, to be able to operate at different angles of attack and Mach numbers, to have good starting and stability characteristics, to create a uniform flow distribution after the appropriate compression system, and have a small, simple and lightweight design. For this purpose, first of all, an air intake design will be performed using computational fluid dynamics (CFD), and then a model of this air intake will be produced with composite materials. In our project, validation studies will be carried out with an air intake comparison problem for which experimental data can be found from the literature. Thus, the suitability of open-source computational fluid dynamics (SU^2 and OpenFOAM etc.) solvers planned to be used will be investigated. Then the CAD model of the air intake will be done using FreeCAD, Salome Platform or similar software, which is an open source software. After the design, production will be carried out by laying and joining method using CFR epoxy composite. It will be developed with technical support from TAI industry consultant on aviation and theoretical support from consultant lecturer. On the other hand, if this project is successful, the capacity of open source-based network generators and solvers for CFD analysis in varying Mach number and angle of attack ranges of composite-based air intake to be used in jet planes will also be measured, and the project team will gain experience in open source software.

1.1 The Purpose of the Thesis

The role of aviation in the national defense industry is of great importance. Since 1974, the national defense industry has accelerated. In recent years, with the developments in the defense industry, new and domestic defense industry products such as Hürkuş and National Combat Aircraft have emerged, and these products have inspired engineering students who are especially keen on aviation. In this context, the project will focus on optimizing composite-based air intakes that can be used in our aircraft, which are the striking power of aviation, according to flight parameters at different angles of attack, and developing a performance model. In line with this goal, the design, miniature production and analysis of an air intake will be carried out using open-source programs that we think will contribute to reducing the foreign

dependency of our country. Experiments and performances of air intakes, which are the main subject of the project, are subjects that have been used for many years and examined with different methods in different time periods. The value to be added here is to contribute to the country in the future by gaining experience in the aviation industry and in fluid dynamics, comparing theoretical calculations and real experiments, by using open-source programs and applications in these air vents, as well as making a study and developing it for a master's degree later on. and to pioneer the possibility of being the subject of a doctoral thesis.

The goal of this thesis;

Design and analysis of classical air intakes used in aviation using open source software according to different angles of attack, as well as examining the effect of side slip angle in addition to the angle of attack, determining the location of the intake on the fuselage, passive control methods to prevent flow separation in the opening (vortex generators). , boundary layer bleed), designing the aperture according to the flight envelope, and finally producing the designed geometry using epoxy composite material.

The main objectives of this graduate project are;

1. Examining the air intakes currently used in line with the given targets and creating the design and necessary parameters using theoretical knowledge.
2. Creating the draft of the air intake with the design and parameters, then creating the CAD model of the determined air intake using open -source software (FreeCAD, Salome Platform).
3. After creating the CAD model, creating the necessary network structure using open-source software (SU^2, OpenFoam) and performing its solution, then comparing the results obtained for a benchmarking problem with the relevant experimental data.
4. Modelling and creating the mold of the air intake. Production by methods such as laying and joining using epoxy composite after it is formed.

1.2 Literature Review

There are many types of air intakes according to their usage areas. Inside the project's parameters, literature research was conducted on high-fidelity computation, air-intake, drag forces and selection of air intake and aircraft.

1.2.1 What is Air Intake?

All turbine engines need an air inlet to function properly. An aviation engine's air inlet is a component that delivers air from the atmosphere to the compressor so it can travel to the engine. The freestream airflow that is brought to the engine offers a sufficient ratio of pressure recovery to air deceleration. The air-inlet duct is typically regarded as an airframe component rather than an engine component. However, the duct is crucial to the engine's overall performance since these properties are essential to the engine's performance and stability as well as its capacity to generate the ideal amount of thrust. The engine's air intake is used to draw air into the engine, which guarantees complete pressure preservation and slows the flow to the compressor at the proper pace so that it may reach the engine face. The performance and stability of the engine's operation depend on these characteristics. This air flow may cross the fuselage before correctly entering the entrance, depending on the air intake design and installation. Any aircraft design must consider how the input geometry and intake type work together.

As a result, one of the most crucial things taken into account during the design phase of an airplane is the air intake design.

1.2.2 Types of Intake

Inlets come in a variety of shapes and sizes with the specifics usually dictated by the speed of the aircraft.

1.2.2.1 Subsonic Inlets

For aircraft that cannot go faster than the speed of sound, like large airliners, a simple, straight, short inlet works quite well. On a typical subsonic inlet, the surface of the inlet from outside to inside is a continuous smooth curve with some thickness from inside to outside.[6] The most upstream portion of the inlet is called the highlight, or the inlet lip. A subsonic aircraft has an inlet with a relatively thick lip, Figure 1, NASA Glenn Research Center; (Inlets (nasa.gov))

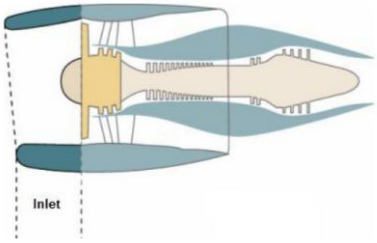

Figure 1 Subsonic Inlet [3]

1.2.2.2. Supersonic Inlets

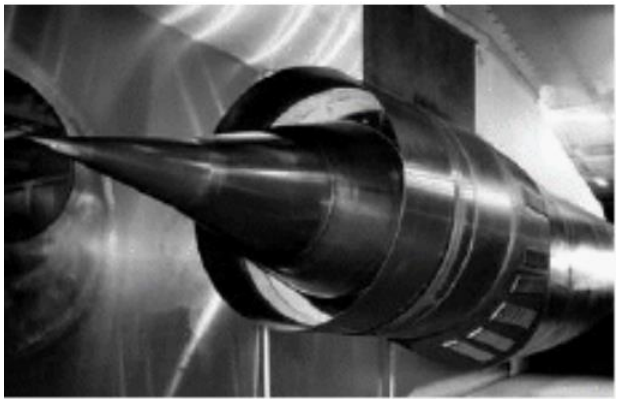

Figure 2 Supersonic Inlet [3]

An inlet for a supersonic aircraft, on the other hand, has a relatively sharp lip. The inlet lip is sharpened to minimize the performance losses from shock waves that occur during supersonic flight. For a supersonic aircraft, the inlet must slow the flow down to subsonic speeds before the air reaches the compressor.[8] Some supersonic inlets, like in the Figure 2, use a central cone to shock the flow down to subsonic speeds. Other inlets, like in the Figure 3, use flat hinged plates to generate the compression shocks, with the resulting inlet geometry having a rectangular cross section. This variable geometry inlet is used on the F-14 and F15 fighter aircraft. More exotic inlet shapes are used on some aircraft for a variety of reasons. The inlets of the Mach 3+ SR-71 aircraft are specially designed to allow cruising flight at high speed. The inlets of the SR-71 actually produce thrust during flight, NASA Glenn Research Center; (Inlets (nasa.gov)) [2]

1.2.2.3 Hypersonic Inlets

For ramjet-powered aircraft, the inlet must bring the high speed external flow down to subsonic conditions in the burner. High stagnation temperatures are present in this speed regime and variable geometry may not be an option for the inlet designer because of possible flow leaks through the hinges. For scramjet-powered aircraft, the heat environment is even worse because the flight Mach number is higher than that for a ramjet powered aircraft. Scramjet inlets are highly integrated with the fuselage of the aircraft. On the X-43A, the inlet includes the entire lower surface of the aircraft forward of the cowl lip. Thick, hot boundary layers are usually present on the compression surfaces of hypersonic inlets. The flow exiting a scramjet inlet must remain super

1.2.3 Drag Forces

The inevitable result of an object traveling through a fluid is drag. Drag is the force that is produced for an object traveling through a fluid that is parallel to and opposing the direction of travel. The resistance created by a body moving through a fluid is known as drag force. In opposition to the direction of the incoming flow velocity, a drag force operates. This is the fluid's and the body's relative velocity. Drag force was employed as a performance measure in this report. The performance of the engine will rise as the drag force decreases since it is inversely proportional to the thrust force of the engine. The downstream component of the pressure and viscous forces acting on the lip and diffuser walls is used to determine drag force.

1.2.4 Pressure Recovery

Referring to Figure 3, the total pressure Pt through the inlet changes, however, because of several flow effects. Aerodynamicists characterize the inlet's pressure performance by the inlet total pressure recovery, which measures the amount of the free stream flow conditions that are "recovered". The pressure recovery $\left(\frac{P_{t2}}{P_{t0}}\right)$ depends on a wide variety of factors, including the shape of the inlet, the speed of the aircraft, the airflow demands of the engine, and aircraft manoeuvres.[3] Recovery losses associated with the boundary layers on the inlet surface or flow separations in the duct are included in the inlet efficiency factor:

$$n_t = \left(\frac{P_{t2}}{P_{t1}}\right) \tag{1}$$

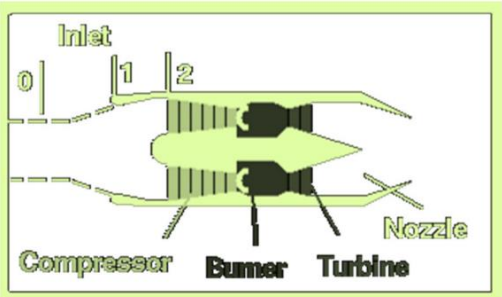

Figure 3 Reference Points of Subsonic Inlet [3]

For subsonic flight speeds, these losses are the only losses. For Mach number Ma less than 1, the Military Specifications (Mil. Spec.) Value of recovery is the inlet efficiency:

At supersonic flight speeds, there are additional losses created by the shock waves necessary to reduce the flow speed to subsonic conditions for the compressor.

The (Mil. Spec.) loss is a good first estimate of inlet recovery. Actual inlet performance may be greater but is usually less than Mil. Spec. The magnitude of the recovery loss depends on the specific design of the inlet and is normally determined by wind tunnel testing.

- For Mil. Spec., M>1:

$$IPR = \left(\frac{P_{t2}}{P_{t0}}\right) = n_i \times (1 - 0.075 \times [M-1]^{1.35}) \quad (2)$$

- For Mil. Spec., M<1:

$$IPR = \left(\frac{P_{t2}}{P_{t0}}\right) = n_i \times 1 \quad (3)$$

Where:

$$n_i = \left(\frac{P_{t2}}{P_{t1}}\right) \quad (4)$$

For hypersonic inlets the value of pressure recovery is very low and nearly constant because of shock losses, so hypersonic inlets are normally characterized by their kinetic energy efficiency. Total pressure recovery (which is the ratio of total pressure at the exit to that at the entry) in subsonic intakes is generally very close to unity and depends primarily on the location of the engine relative to the airframe. For example, the intake of an engine located on the wing (like the Boeing 777) would have a relatively obstruction free flow leading to high pressure recovery, while, that for an engine located at the vertical tail (e.g. Boeing 727) would not be able to perform as well.

1.2.5 Spillage Drag

There is an additional propulsion performance penalty charged against the inlet called spillage drag. Spillage drag, as the name implies, occurs when an inlet "spills" air around the outside instead of conducting the air to the compressor face. The amount of air that goes through the inlet is set by the engine and changes with altitude and throttle setting. The inlet is usually sized to pass the maximum airflow that the engine can ever demand and, for all other conditions, the inlet spills the difference between the actual engine airflow and the maximum air demanded. As the air spills over the external cowl lip, the air accelerates and the pressure decreases. This produces a lip suction effect that partially cancels out the drag due to spilling. Inlet aerodynamicists account for this effect with a correction factor K that multiplies the theoretical spillage drag. Typical values of K_f range from .4 to .7. But for a given inlet the value is determined experimentally. The form of the theoretical spillage drag D spill is very similar to

the thrust equation, with a mass flow m dot times velocity term V and a pressure p times area A term:

$$D_{spill} = K_f \dot{m}(V_1 - V_0) + A_1(P_1 - P_0) \quad (5)$$

1.2.6 Air Intake Selection

The main purpose of the air intake is to slow the airflow through the compressors until it reaches supersonic flight speed to necessary subsonic speed. The component of an airplane's construction known as the air intake is used to supply air from the outside atmosphere to the aircraft engine. Simply put, the pitot entry is a hole that faces forward. At modest supersonic speeds, it performs admirably and very well at subsonic speeds. When employed for supersonic flight, it is often referred to as "normal shock absorption". Lip and diffuser components make up the pitot air intake. Pitot Type air intakes are designed to give engines a smooth airflow that is between Mach 0.4 and 0.5.

Figure 4 Pitot-type nose, side and center-body air inlets

It does not produce oblique shock, unlike air inlets that are ramped or conical. In a single conventional shock, it seeks to decelerate the supersonic flow. Among the compared geometries, it is the lightest and least complex in terms of design. Because of this, it is preferred in terms of output if it effectively recovers pressure. There must be more than one shock wave produced in order to cruise at Mach 1.6 and higher Mach values. Air intakes with ramp openings should therefore be preferred. As a result, for reasons of simplicity and lightweight, the majority of jets made for speeds below Mach 1.6 have a pitot intake.

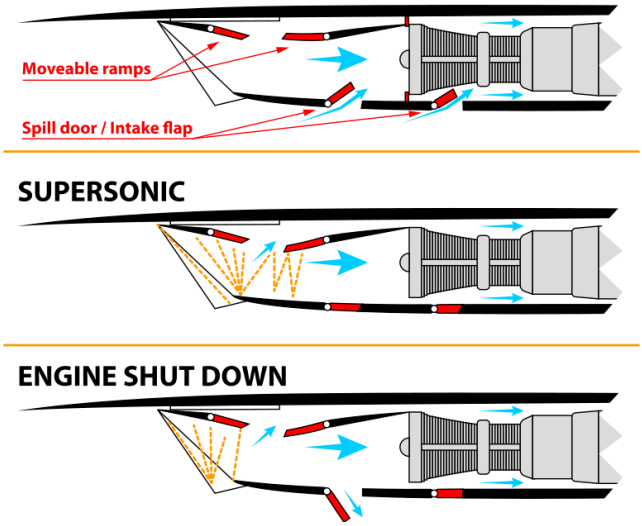

Figure 5 Air Intake Ramp

1.2.7 Compression Ramp

A rectangular, plate-like device called an intake ramp or compression ramp is used in the air intake of jet engines to help the inlet compression process at supersonic speeds by producing a number of shock waves. In order to divert the intake air from the longitudinal direction, the ramp is positioned at an acute angle. At each gradient change along the ramp, the bending of the air stream at supersonic flight speeds produces a series of oblique shock waves. The pressure rises as air passing through each shock wave abruptly slows to a lower Mach number.

The air intake lip should ideally be caught by the first oblique shock wave to prevent air leakage and pre-entry drag on outer boundary of the deflected stream tube. Because the angle of the shock wave (to the longitudinal direction) gets more severe with rising aircraft speed, this condition can only be met for a fixed shape intake at zero incidence for a specific flight Mach number.

The ramp in more sophisticated supersonic intakes has numerous discrete gradient adjustments to produce multiple oblique shock waves. In the case of Concorde, a diverging intake ramp comes after the initial (converging) intake ramp. After the first ramp's conclusion, the air has already reached subsonic speed, therefore the diverging ramp helps to further slowdown the airstream and, as a result, raise its pressure. By ensuring great pressure recovery through this intake design, Concorde is able to cruise supersonically at up to Mach 2.2 and achieve enhanced fuel efficiency (beyond which airframe heating effects limit any further increase in speed).

Intakes with variable geometry, like those on Concorde, change the ramp angle to focus a series of oblique shock waves onto the intake lip. The ramp void pressure which is the pressure

of the air between the two ramps is used as a control input for these complex non-linear control laws, which are used to control the intake geometry.

The input cone for circular intakes is the counterpart of the intake ramp for rectangular intakes. On newer aircraft, which are designed with a greater emphasis on durability and survival, much lighter fixed-geometry substitutes are utilized. By regulating shock location using the downstream pressure, these inlets maintain the performance of changing intake ramps. These include the diverterless supersonic inlet used on the Lockheed Martin F-35 Lightning II and Chengdu J-20, as well as the caret compression surface used in the Lockheed Martin F-22 Raptor and Boeing F/A-18E/F Super Hornet inlets.

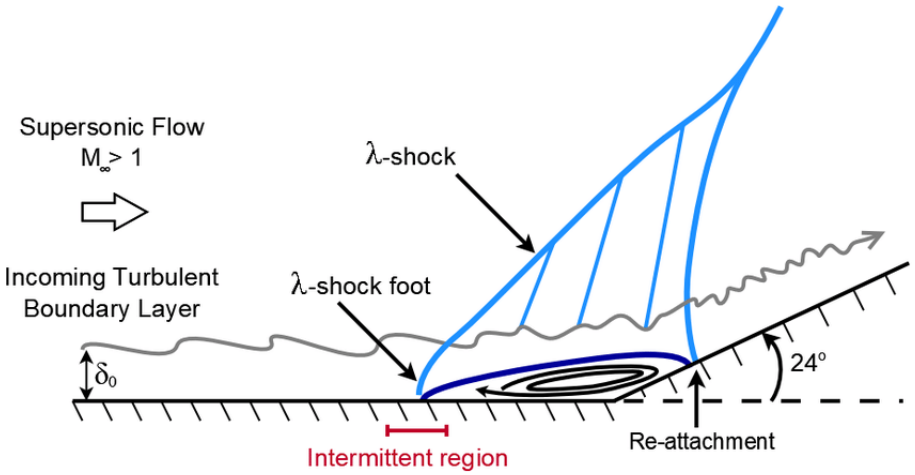

Figure 6 The flow over a compression ramp

1.2.8 Serpentine Inlet (S-Duct)

A typical style of intake for jet engines is the S-duct. An intake is needed for all jet engines. It is in charge of catching and slowing down air before it enters the combustion chamber of the engine; it is also known as an intake. Although there are numerous varieties of jet engine intakes, the S-duct is one of the most popular. However, S-duct intakes have benefits and drawbacks much as other forms of intakes.

Shorter fins are possible with S-duct intakes. Stabilisers are the fins. They are made up of tiny wings-like flight control surfaces, which are intended to increase flight stability. An S-duct intake eliminates the requirement for a long fin on aircraft. Instead, they could be given a short fin. Engine location is a benefit of S-duct intakes as well. In actuality, the S-duct was initially created for trijet engine arrangement. Three jet engines are used to power trijet aircraft. In the event that an aircraft only has two jet engines, one of them will normally be located on either side of the fuselage. Trijets, on the other hand, need an alternative approach because they have an odd number of jet engines. Trijets can have their third jet engine in the middle thanks to D-

duct intakes. Compared to other types of jet engine intakes, S-duct intakes are simpler. For instance, certain trijets have straight-through intakes for each of their individual jet engines. Straight-through intakes are higher up, making it challenging to get to them. Because S-duct intakes are lower, engineers and maintenance personnel may easily access them. S-duct intakes reduce drag more than straight-through intakes do in an aircraft. According to some sources, an S-duct input can reduce drag by as much as 4%. Additionally, airplanes are more effective with less drag. They can travel farther while using less gasoline.

The price of S-duct intakes is one of their main downsides. Compared to most other types of jet engine intakes, they are more expensive to construct and install. More work goes into the S-duct intake than the straight-through intake. And because of its intricate design, it is more expensive to make and install. S-duct intakes are uncommon on commercial aircraft. Jet engines are typically installed in even numbers on commercial aircraft. Some of them are equipped with two jet engines, while others have four. Contrarily, trijets, which have three jet engines, frequently use S-duct intakes.

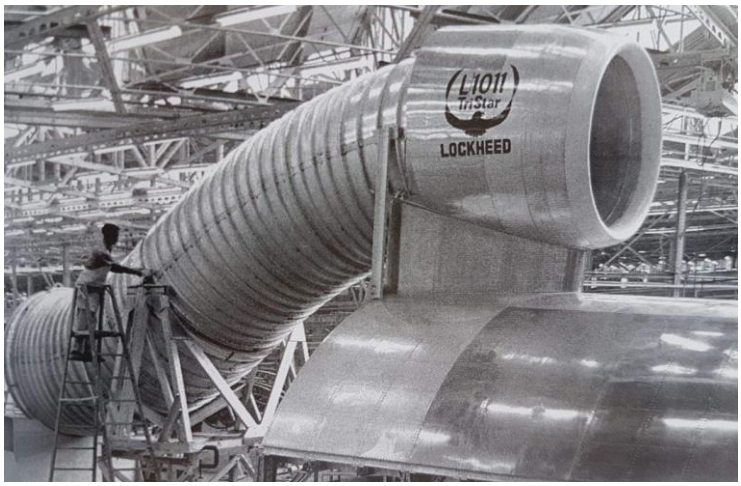

Figure 7 S-duct of jet engine

1.2.9 RAE M2129 Intake

An S-duct diffuser, named RAE M2129, was designed around 1990 under a joint program between NASA and the UK defense Ministry and was tested in the DRA/Bedford 13x9 ft wind tunnel. A large number of diffuser geometries have been studied with different lip shapes, cross-sectional changes, and etc.

Geometry of RAE M2129 intake can be divided into three main parts. These are cowl, diffuser (s-duct) and engine aerodynamic interface plane (AIP). The intake has circular cross sections from beginning to end, and the cross sections are constant for a diameter upstream of throat and a diameter downstream of diffuser. Constant cross sections are connected with serpentine

diffuser. Cowl of the intake is an ellipse with ¼ ratio. Curve of centerline for serpentine diffuser and distribution of radius can be obtained with following equations [1];

$$Z_{cl} = -\Delta Z\left[1 - cos\frac{\pi X_{cl}}{L}\right]\frac{R - R_i}{R_{ef} - R_i} = 3\left(1 - \frac{X_{cl}}{L}\right)^4 - 4\left(1 - \frac{X_{cl}}{L}\right)^3 + 1 \qquad (6)$$

with parameters as given below;

$$R_1(Throat\ Radius) = 0.0644\ m$$

$$\frac{R_{ef}}{R_1} = 1.183$$

$$\frac{L}{R_1} = 7.1$$

$$\frac{\Delta Z}{R_1} = 2.13$$

2. ASSISTANT SOFTWARES

2.1 MATLAB

Engineers and scientists can use the programming environment MATLAB to study, create, and test systems and technologies that will change the world. The MATLAB language, a matrix-based language that enables the most natural expression of computer mathematics, is the core of MATLAB. MATLAB software is used to make some calculations.

2.2 MS Excel

One often used Microsoft Office program is MS Excel. The application is a spreadsheet that is used to store and analyse numerical data. MS Excel is used to systematically read and organize data.

2.3 SALOME Platform

A multi-platform open source scientific computing environment called SALOME enables the execution of commercial research of physics simulations. SALOME offers the computational environment required for their integration but does not itself contain a physics solver. The SALOME environment serves as the foundation for the development of disciplinary platforms, including SALOME-HYDRO, Salome meca, and Salome cfd.

SALOME Platform is used to draw CAD model of the geometries that we used in project. And also it is used to make a proper mesh for computational fluid dynamics (CFD) solver.

2.4 SU^2

SU^2 is a collection of free and open-source C++ software tools for solving partial differential equations (PDE) numerically and carrying out PDE-restricted optimization. Although it has been expanded to include more general equations like electrodynamics and chemically reactive flows, computational fluid dynamics and aerodynamic form optimization remain the main applications. For determining the sensitivities/gradients of a scalar field, SU^2 allows both continuous and discrete adjoint**.**

SU^2 is used as computational fluid dynamics (CFD) solver for our project.

3. SUBSONIC VERIFICATION STUDY

3.1 CAD MODEL

The CAD model was build based on the RAE M2129 Intake geometry. The s-duct part sliced into 25 pieces, the diameter at these points were calculated, then by interpolating with these circles, geometry was created.

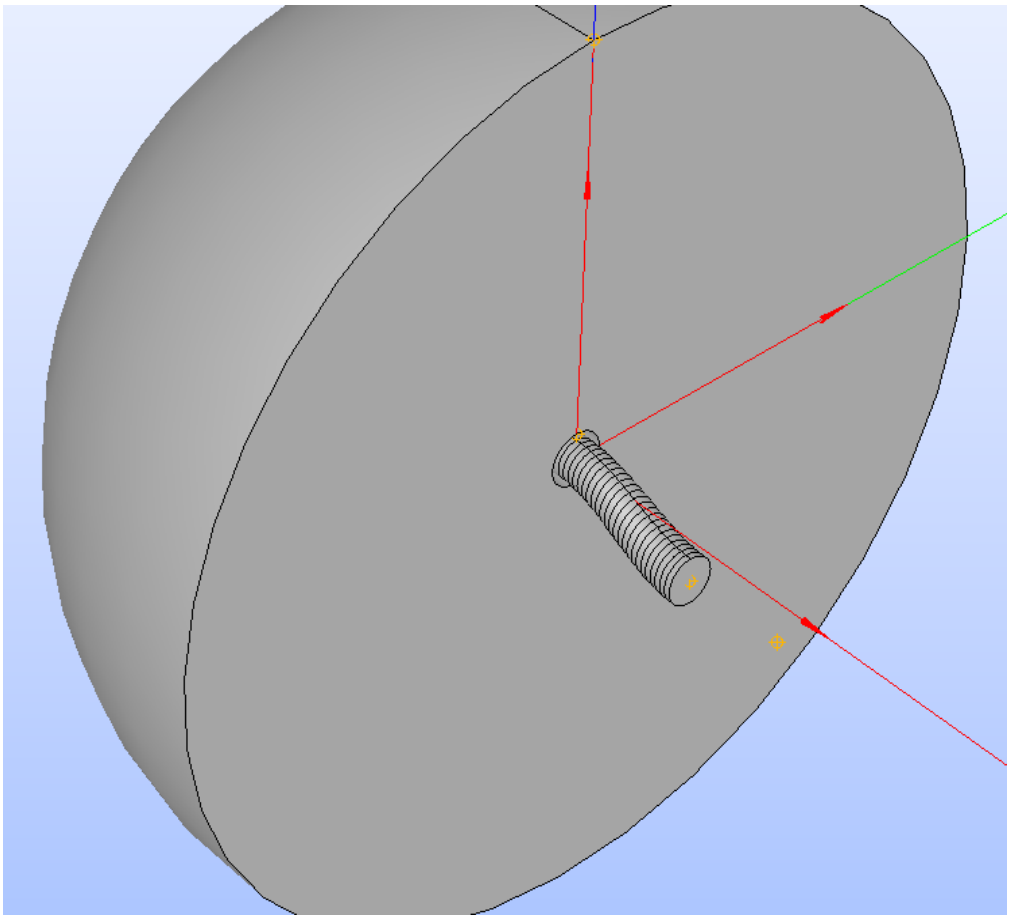

Figure 8 RAE M2129 geometry

3.2 MESH

NETGEN 1D-2D-3D is used as a algorithm. NETGEN 3D is used as hypothesis with max. size of 0.25 m and min. size of 0.005 m. And also local size is used to create more proper mesh with 0.005 m. Viscous Layers is used as a additional hypothesis with total thickness of 0.01m and 40 layers. 'Surface offset + smooth' is used as a extrusion method. Y+ value is between 1-3.

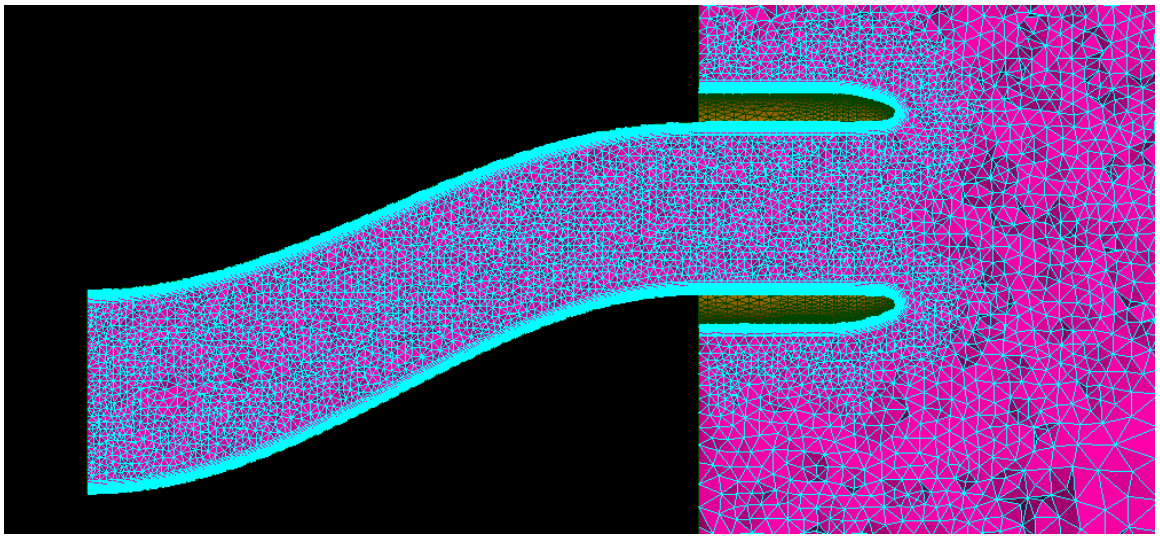

Figure 9 Section view of mesh structure

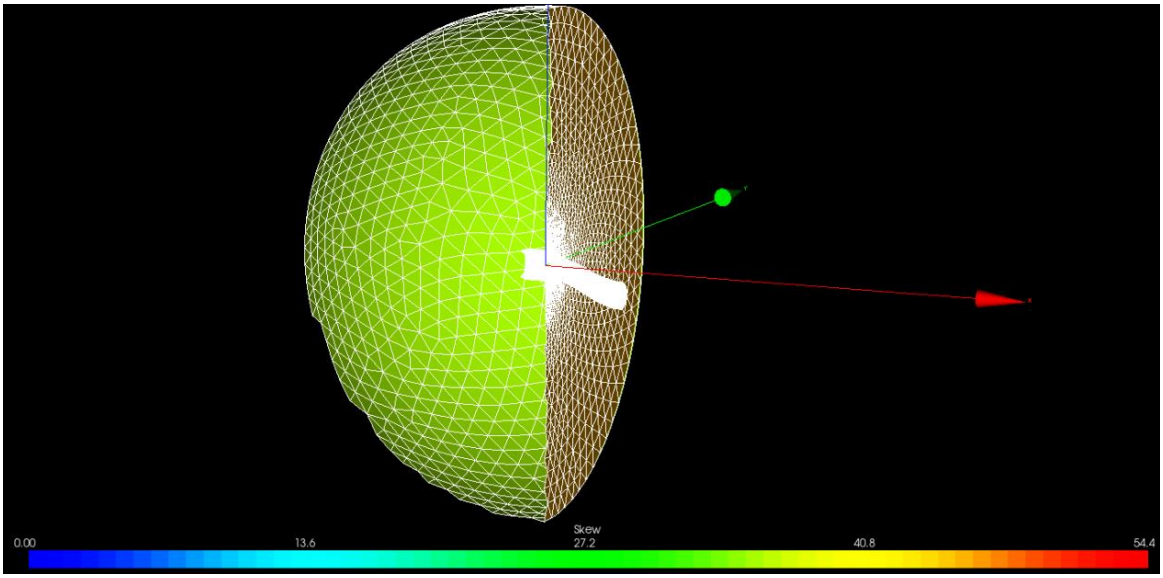

Figure 10 Section view of mesh structure

Base Info	Element Info	Additional Info	Quality Info		
Name:	Mesh_1				
Object:	Mesh				
Nodes:	739275				
Elements:	*Total*	*Linear*	*Quadratic*	*Bi-Quadratic*	
	2146300	2146300	0	0	
0D:	0				
Balls:	0				
1D (edges):	4016	4016	0		
2D (faces):	43758	43758	0	0	
Triangles:	*37158*	*37158*	*0*	*0*	
Quadrangles:	*6600*	*6600*	*0*	*0*	
Polygons:	*0*	*0*	*0*		
3D (volumes):	2098526	2098526	0	0	
Tetrahedrons:	*981926*	*981926*	*0*		
Hexahedrons:	*0*	*0*	*0*	*0*	
Pyramids:	*0*	*0*	*0*		
Prisms:	*1116600*	*1116600*	*0*	*0*	
Hexagonal Prisms:	*0*				
Polyhedrons:	*0*				

Figure 11 Mesh Information

3.3 RESULTS AND VERIFICATION

Pressure far-field boundary condition is assigned to surfaces of the imaginary field. Mach number was determined as 0.207, freestream pressure was determined as 100018.8 Pa, freestream temperature was determined as 280.2 K and Reynolds number based on the free-stream was determined as 0.707×10^6. Iterations were continued until the rms values decreased to 10^{-8}.

The comparison was made with Mach number and pressure recovery values. The variations were made with controlling the back pressure at the constant mass flow rate. The turbulence models and results we solved:

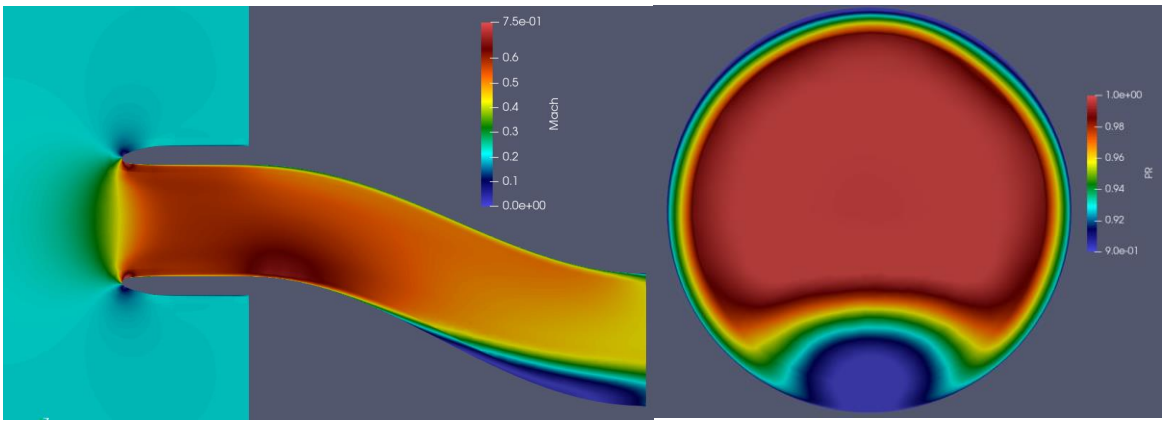

Figure 12 Mach contours and Pressure Recovery at AIP (CFD-1)

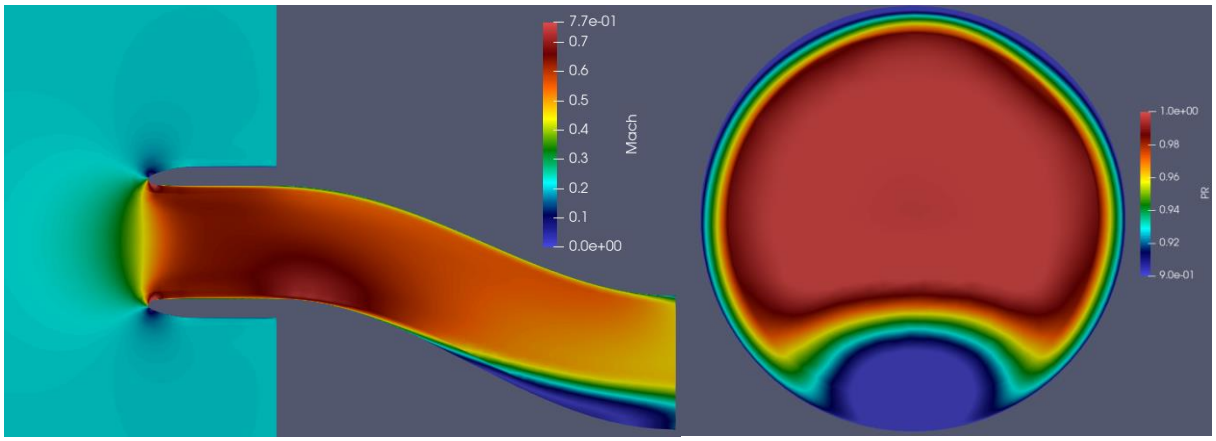

Figure 13 Mach contours and Pressure Recovery at AIP (CFD-2)

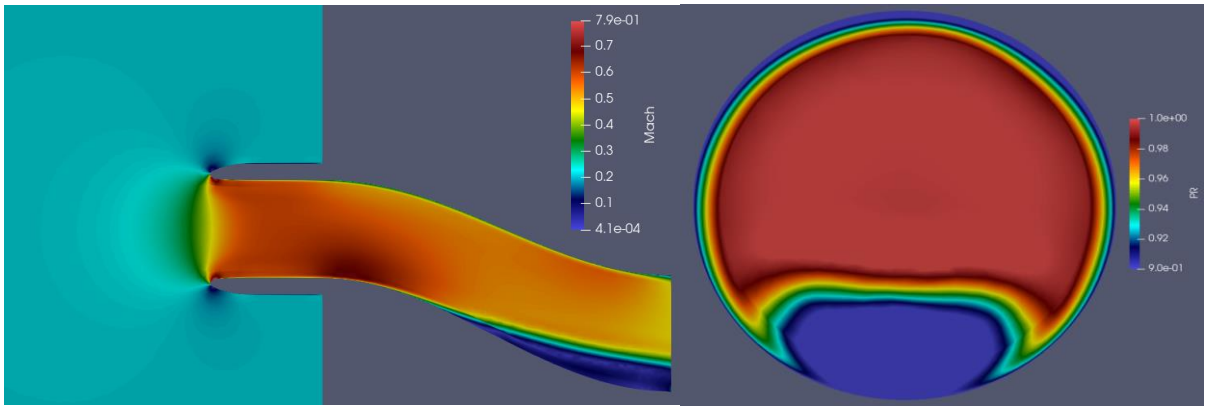

Figure 14 Mach contours and Pressure Recovery at AIP (CFD-3)

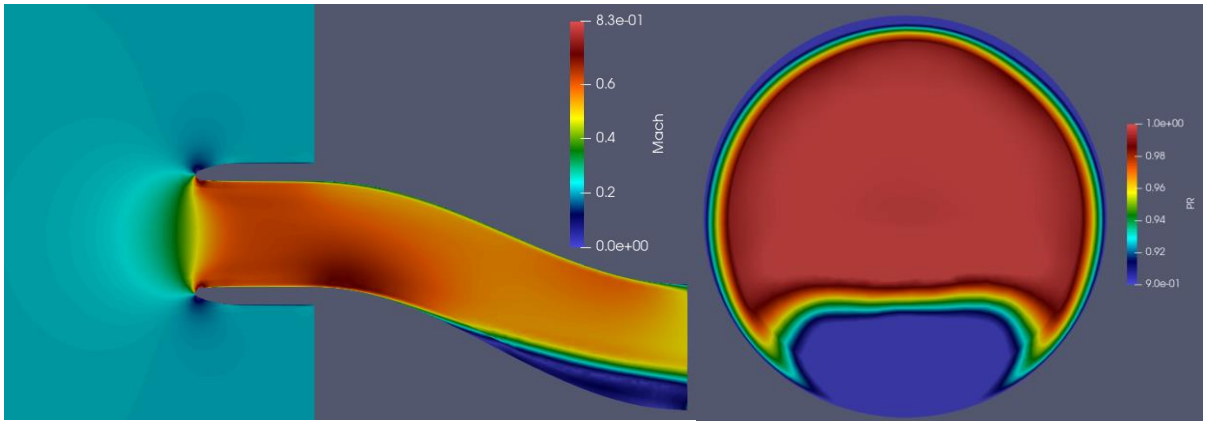

Figure 15 Mach contours and Pressure Recovery at AIP (CFD-4)

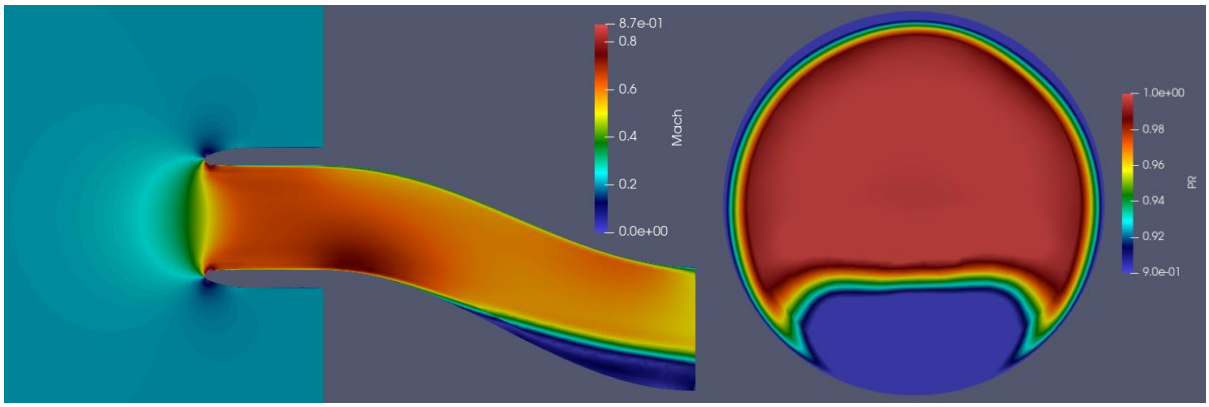

Figure 16 Mach contours and Pressure Recovery at AIP (CFD-5)

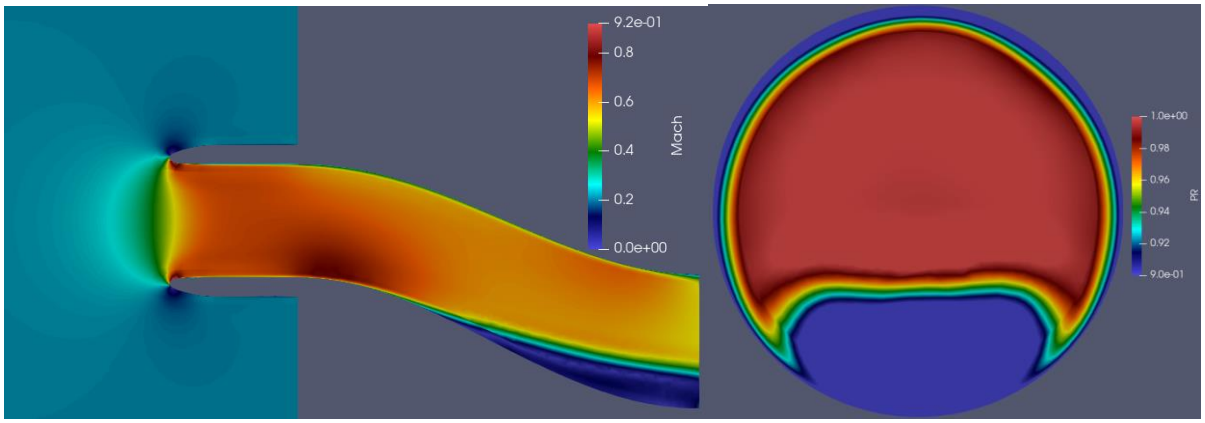

Figure 17 Mach contours and Pressure Recovery at AIP (CFD-6)

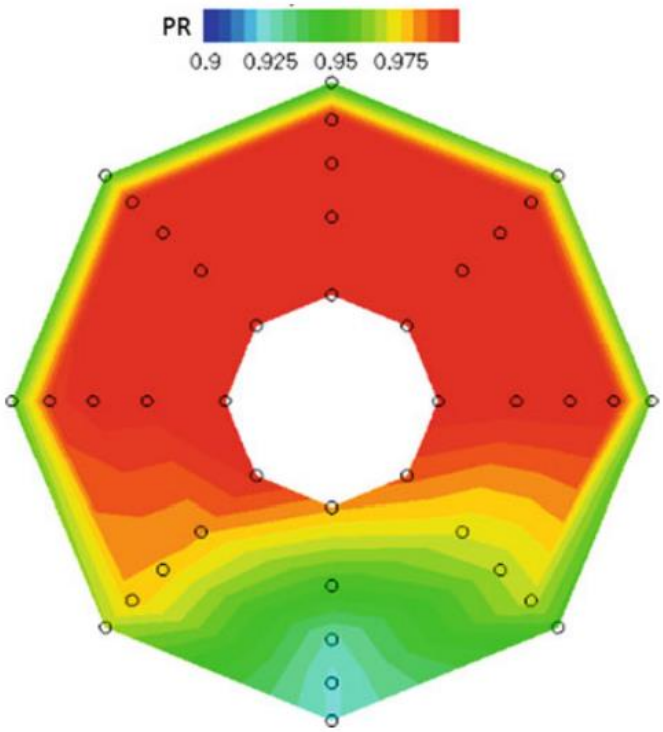

Figure 18 Experimental Result of Pressure Recovery at AIP[4]

A summary of the CFD solutions and experimental results is given in the table below. Errors between experimental results and CFD solutions is calculated.

Table 1 Results of CFD Calculations

	Back Pressure (Pa)	Turbulence Model	Pressure Recovery	Mach	Mass Flow Rate (kg/s)	PR Error	Mach Error	MFR Error
Experiment	-	-	0,9798	0,395	2,873	-	-	-
CFD-1	90674	SST+Vorticity	0,9756	0,379	2,611	0,00429	-0,0405	0,0912
CFD-2	89079	SST	0,9715	0,402	2,73	0,00847	0,0177	0,0498
CFD-3	88800	SA	0,9678	0,394	2,649	-0,0122	0,00253	0,0780
CFD-4	87750	SA	0,9646	0,408	2,71	-0,0155	0,0329	0,0567
CFD-5	86500	SA	0,9606	0,423	2,775	-0,0196	0,0709	0,0341
CFD-6	85000	SA	0,9556	0,441	2,844	-0,0247	0,116	0,0101

Rms and mass flow rate values of the CFD-1 which has least PR error are shown in graphics below.

Figure 19 Log10 of the Residuals vs Iterations

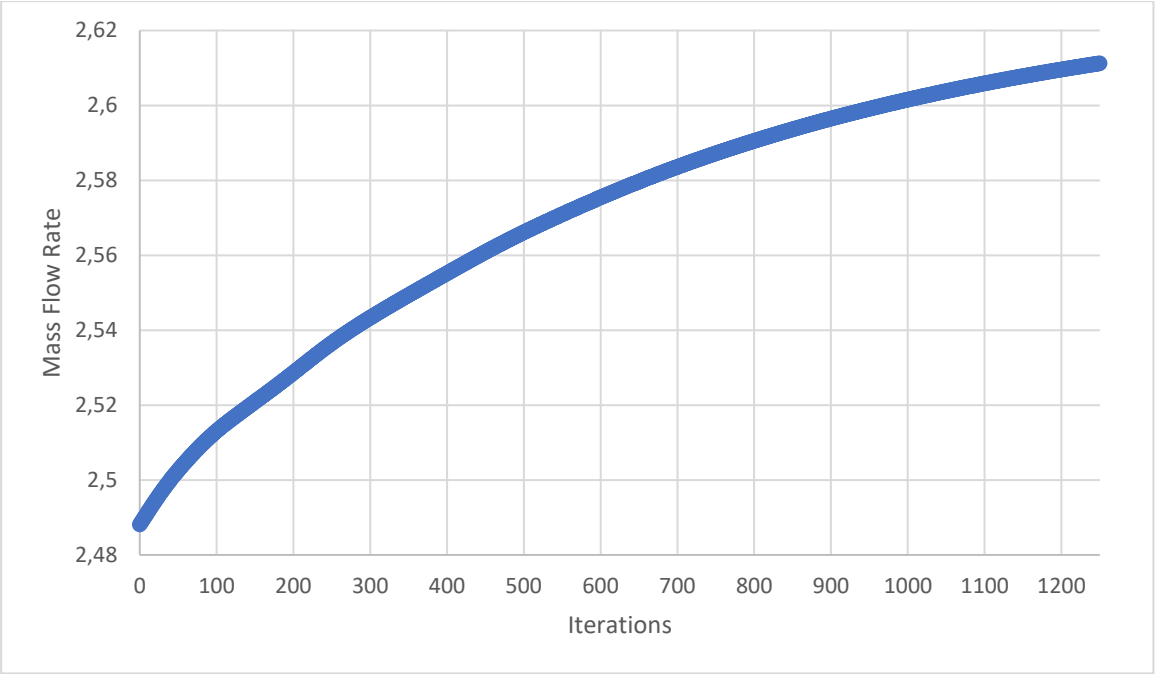

Figure 20 Mass Flow Rates vs Iterations

3.4 MESH INDEPENDENCY STUDY

In our numerical study with finite volumes method, the quality of the mesh structure affects the accuracy of the results. As the geometry became more complex, it became more difficult to improve the mesh quality. Therefore, a mesh independence study was conducted to validate our study. As shown below, 2 more mesh structures were obtained by increasing or decreasing certain parameters by 33 percent and the results were compared.

Table 2 Mesh Parameters

Parameters	Normal	Coarse	Fine
Max. Size(m)	0.25	0.3325	0.1675
Min. Size(m)	0.005	0.00665	0.00335
Growth Rate	0.05	0.05	0.05
Nb. segs per edge	5	3	7
Nb. segs per radius	7	5	9
Hemisphere local size(m)	0.25	0.3325	0.1675
sduct local size(m)	0.005	0.00665	0.00335
Total Thickness(m)	0.01	0.0133	0.0067
Nb. of layers	40	40	40
Stretch factor	1.15	1.15	1.15
Nodes	739275	455054	1628056
Elements	2146300	1401882	4702923
Max. Skewness	54.4	61.5	47.2
Y+	1_3	3_4	1
Pressure Recovery	0.9756	0.9754	0.976
Mach	0.379	0.379	0.379
Mass Flow Rate(kg/s)	2.611	2.613	2.612
PR Error (%)	-0.428659	-0.449071	-0.387834
Mach Error (%)	-4.05063	-4.05063	-4.05063
MFR Error (%)	-9.11939	-9.04977	-9.08458

As seen in table above, it was observed that the outputs of the CFD analysis changed slightly when the mesh structure was changed. Within the scope of this study, grid convergence indices were calculated.[10]

The order of convergence was determined.

$$p = \ln\left[(0.9754)/(0.9756 - 0.976)\right]/\ln(1.33) = 2.4306$$

Richardson extrapolation was applied to obtain an estimate of the value of the pressure recovery.

$$PR_{h=0} = 0.976 + (0.976 - 0.9756)/2^{2.4306-1} = 0.9761$$

The GCI for fine and normal mesh is

$$GCI = 1.25|(0.976 - 0.9756)/0.976)/2^{2.4306-1}|x100 = 0.0117\ \%$$

The GCI for normal and coarse mesh is

$$GCI = 1.25|(0.9756 - 0.9754)/0.9756)/2^{2.4306-1}|x100 = 0.0058\ \%$$

According to results, it was assumed that the CFD analyses were performed independently of the mesh.

4. SUPERSONIC VERIFICATION STUDY

4.1 CAD MODEL

In order to validate supersonic geometry, we designed mixed-compression supersonic inlet. Geometry was designed according to article Zhuoran Liu, Caizheng Wang, Ke Zhang, Zhuo Zhao, Zhifeng Xie (2021) Research on Computational Method of Supersonic Inlet/Isolator Internal Flow, China which has experimental results.

The geometry was created on Salome Platform by following the measurements at Figure 21.

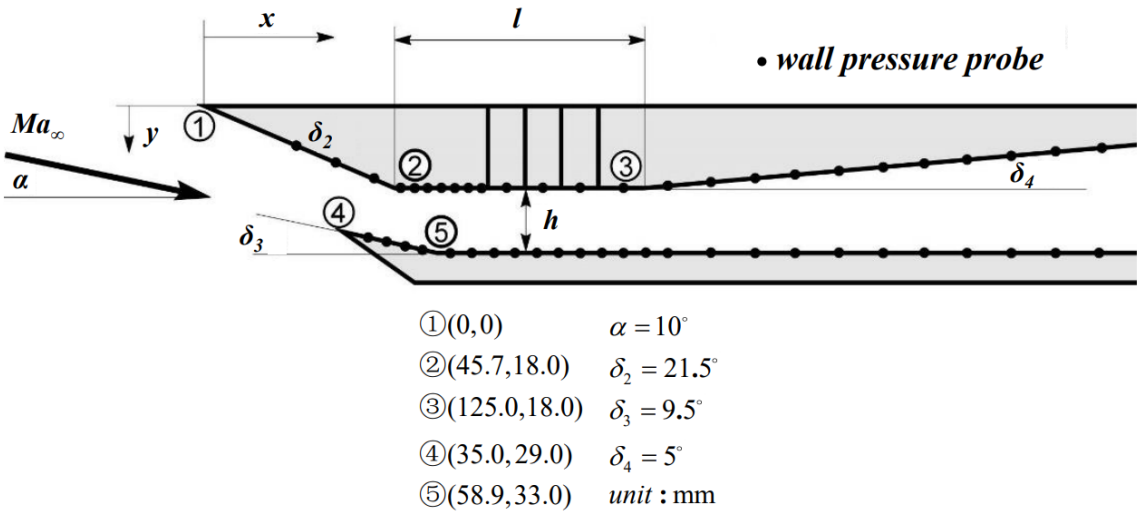

Figure 21 Reference 2D geometry [7]

After the geometry created, the far field created by the radius twice of the entry length.

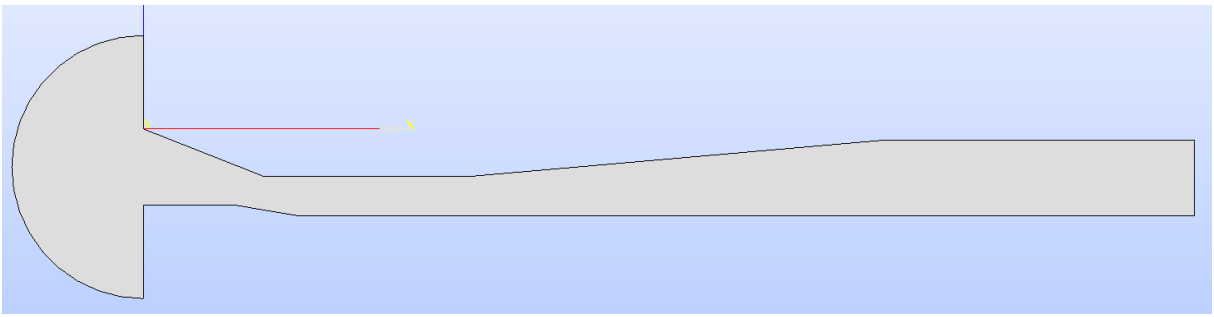

Figure 22 Mixed-compression Inlet

4.2 2D – MESH

To accurately capture the near-wall flow characteristics, a refined mesh is employed in the immediate vicinity of solid surfaces, especially near walls and regions of significant flow gradients. The goal was to achieve the value of the Y+ equal to 1. It may be seen that the mesh is coarser at the far field.

While emphasizing boundary layer resolution, the mesh also ensures adequate resolution in the far-field region. Coarser mesh elements are utilized away from the boundaries, where gradients and complexities are lower. This balanced approach optimizes computational resources while capturing the overall flow features and large-scale turbulence structures accurately.

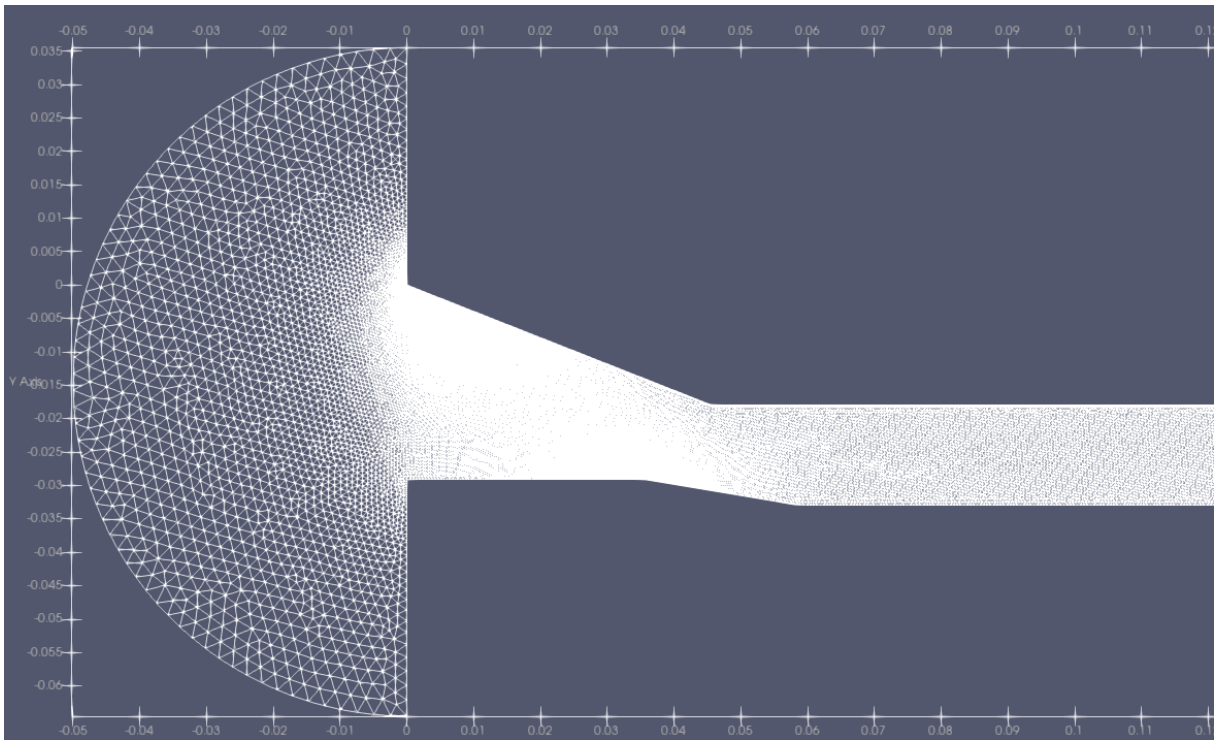

Figure 23 Grid structure

4.3 RESULTS AND VERIFICATION

Supersonic flows often exhibit adverse pressure gradients, particularly near shocks or flow separations. The Spalart Allmaras model's formulation includes an improved treatment of adverse pressure gradients, enabling better prediction of flow separation and shock wave interactions commonly encountered in supersonic regimes. The model was solved by using Spalart–Allmaras model with using SU^2 software.

Pressure far-field boundary condition is assigned to surfaces of the imaginary field. Supersonic outlet boundary condition is assigned to duct exit. Mach number was determined as 2.4, freestream pressure was determined as 36935.657 Pa, freestream temperature was determined as 141.73 K and Reynolds number based on the free-stream was determined as 15.07×10^7. Iterations were continued until the rms values decreased to 10^{-8}.

It can be seen from Figure 24 that the wave system inside the intake duct is highly complicated. The oblique shocks are reflected multiple times inside the isolator. Moreover, the oblique shocks interact significantly with both shock waves and expansion waves, as well as with turbulent boundary layers. These interactions result in noticeable flow separations occurring near the throat of the inlet.

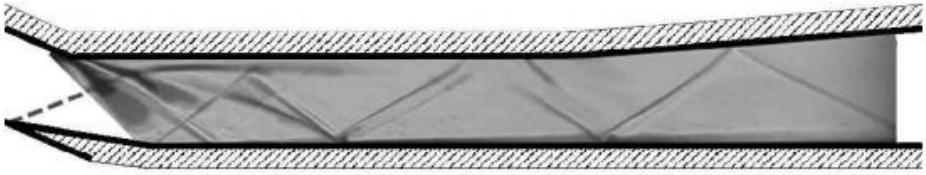

Figure 24 Experimental schlieren picture [9]

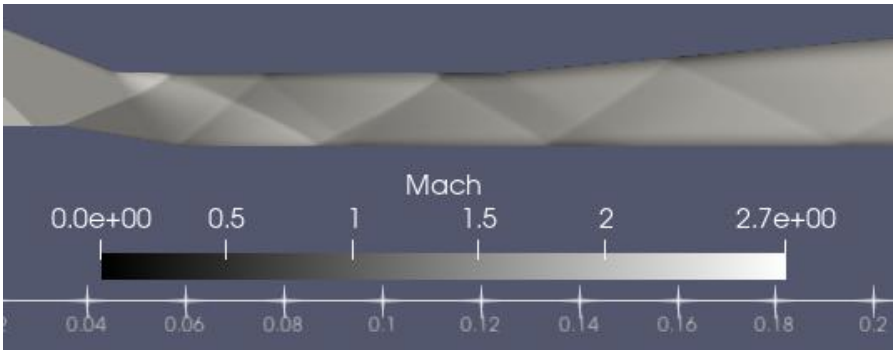

Figure 25 Computational Mach Contour

In the study conducted by Herrmann et al. [9] a comparison was made between the experimental results and the numerical results obtained through computational analysis. The objective was to evaluate the accuracy and reliability of the numerical simulations by assessing their agreement with the experimental data.

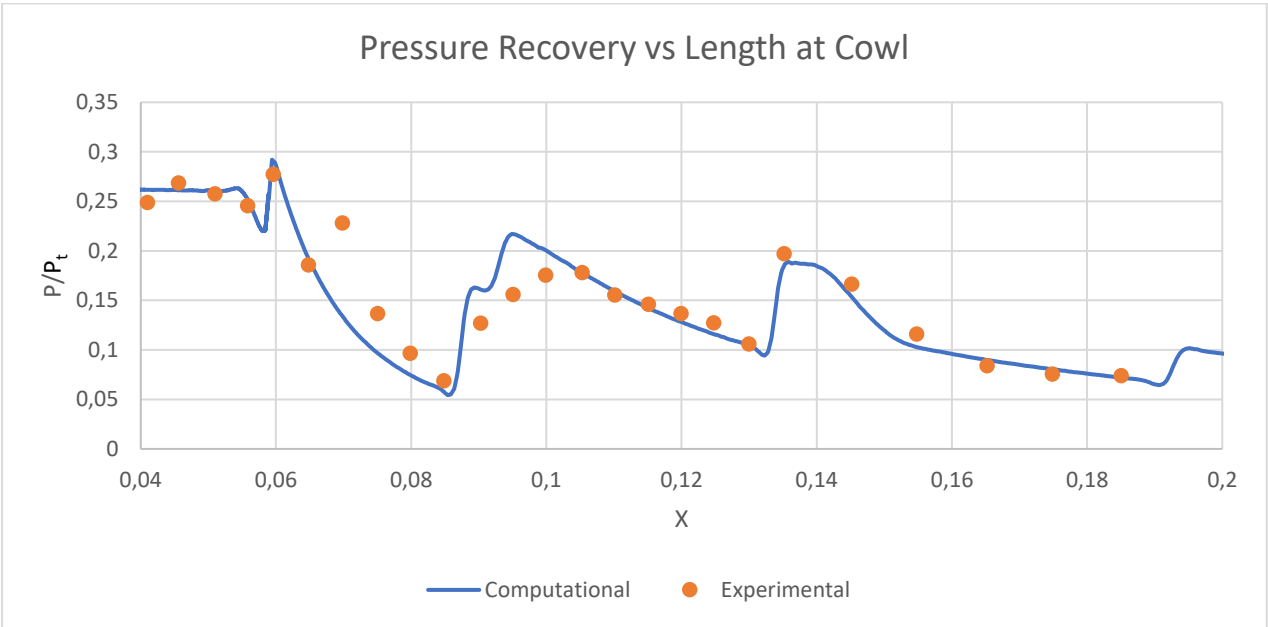

Figure 26 Comparison of experimental results [9] at cowl

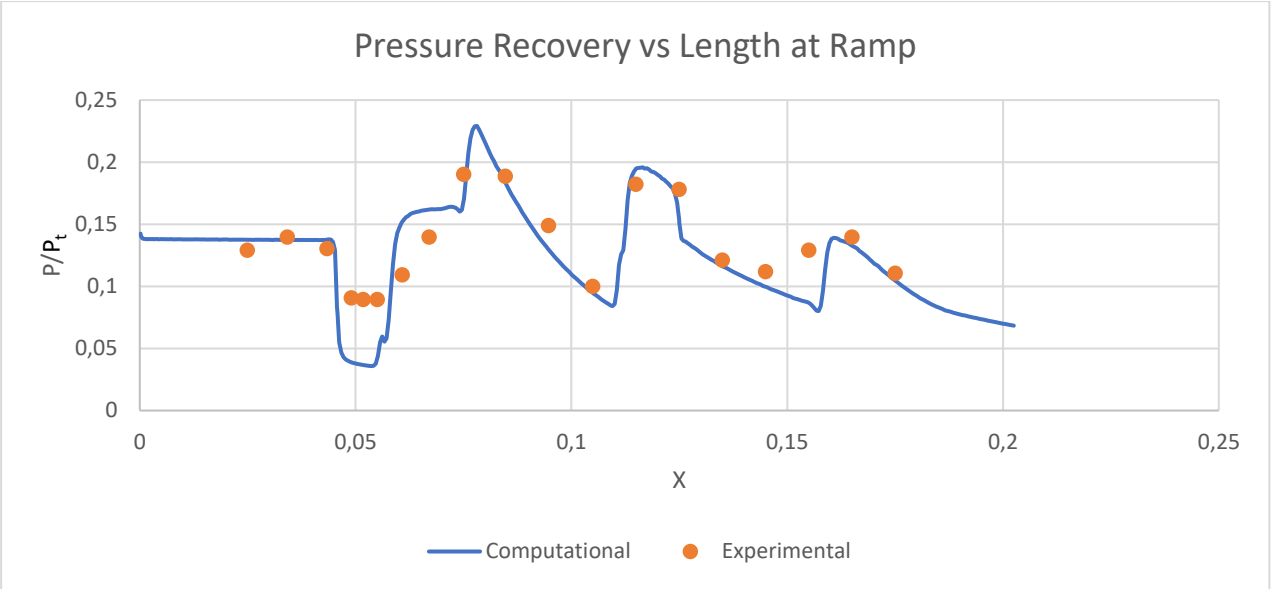

Figure 27 Comparison of experimental results [9]at ramp

The comparison of results at the cowl and the ramp demonstrated a successful alignment. Numerical results provide confidence in the accuracy and applicability of the computational model used in the study. It supports the verification that model and software will be used.

5. DESIGN

5.1 MOLD DESIGN

It is planned to use "Carbon Fiber Reinforced" material, which is a material advantageous in terms of weight and high strength, for the production of the air intake. It is planned to use long-lasting and high-temperature resistant epoxy as the resin.

The mold is designed at an angle so that the air intake can easily come out of the mold. Although this design reduces efficiency, it provides convenience in terms of production. It reduces the production cost. Mold design consists of 3 parts.

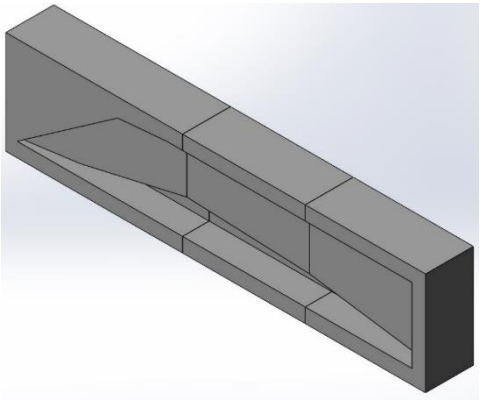

Figure 28 Mold CAD Model

Pressure far-field boundary condition is assigned to surfaces of the imaginary field. The analysis of geometry conducted at Mach numbers between 0.2 and 2, freestream pressure was determined as 36935.657 Pa, freestream temperature was determined as 141.73 K and Reynolds number based on the free-stream was determined as 0.707×10^{6}. Iterations were continued until the rms values decreased to 10^{-8}.

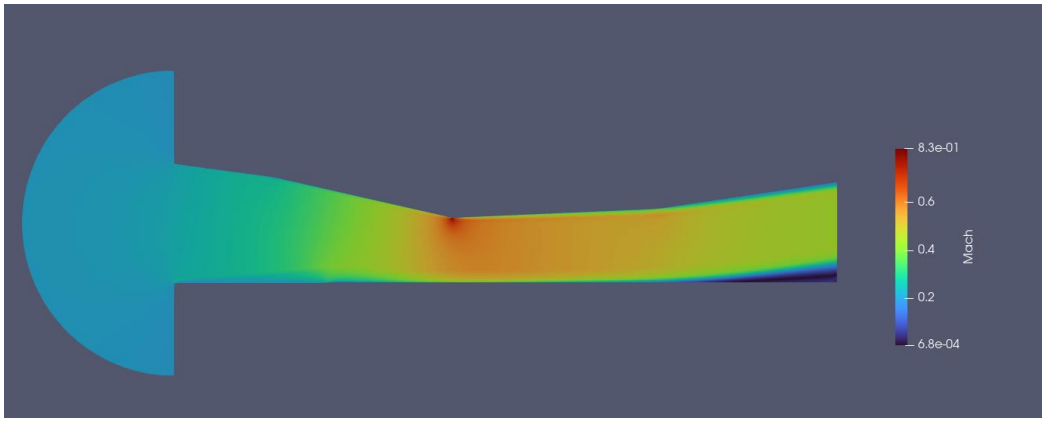

Figure 29 0.2 Mach Result

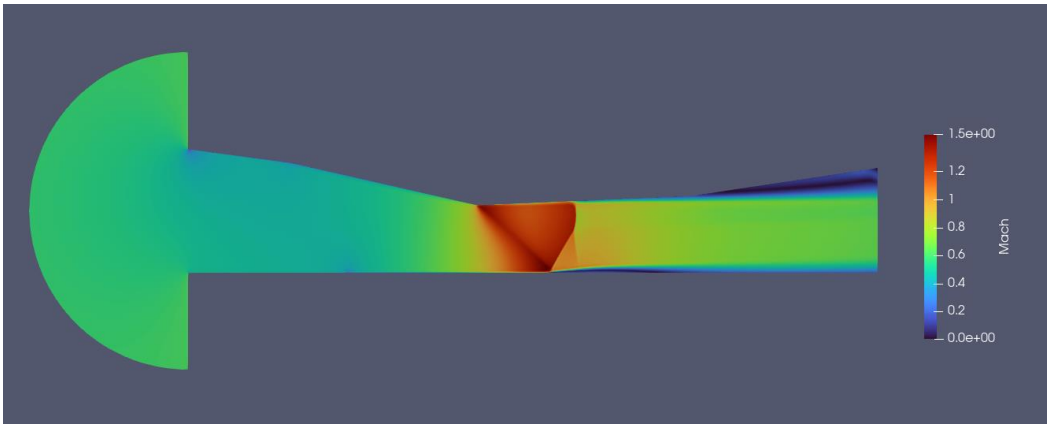

Figure 30 0.6 Mach Result

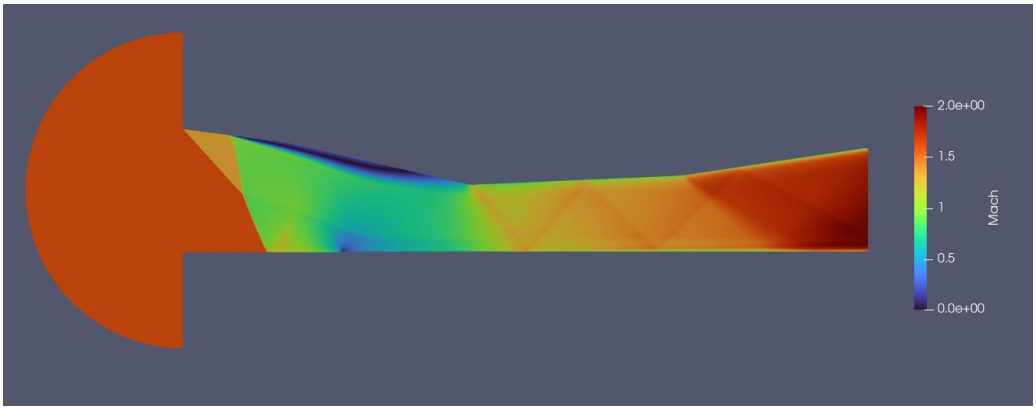

Figure 31 1.6 Mach Result

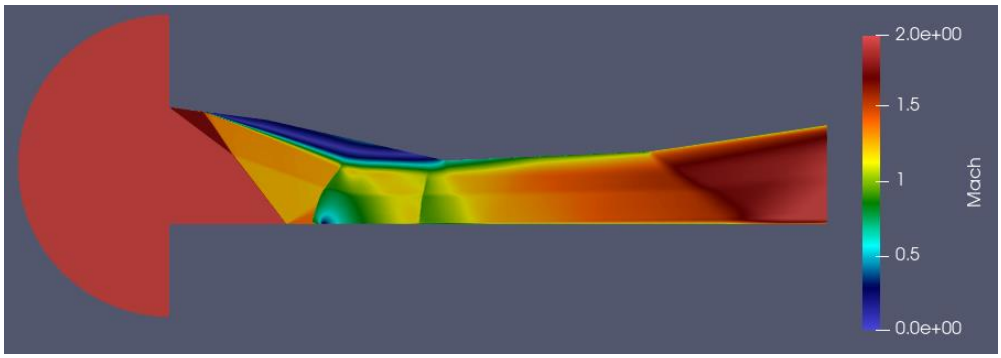

Figure 32 2.0 Mach Result

According to result of the CFD analysis, the supersonic results were better. Even though seen at Figure 30 0.6 Mach Result, the flow is chocked in the narrowest part of the designed air intake, it is designed for supersonic flow. It can be improved with considering subsonic part on the further research.

6. CONCLUSION AND FUTURE WORK

To conclude, the project's investigation of variations in composite-based air inlets with various outlet pressures and Mach numbers, which may be employed in our aircraft as supersonic and subsonic components while taking flight factors into account, is the main emphasis. Using open-source software, the design, small production, and analysis of an air intake were made possible. The primary focus was, the tests and air inlet performance, has been investigated for many years utilizing a variety of techniques over a wide time span.

In the subsonic air intake, the results shows that the best turbulence model is SST + Vorticity model with the pressure recovery error 0,00429 which is closest to the experiment results [5]. The other variables obtained with this analysis are pressure recovery 0,9756, Mach number 0,379, mass flow rate 2,611, Mach error -0,0405, mass flow rate error 0,0912.

At the supersonic air intake, the goal was to determine how precisely the numerical simulations agreed with the experimental data in order to assess their correctness and reliability. The comparison of the findings at the cowl and the ramp showed that the alignment was successful. The correctness and applicability of the computational model utilized in the study are confirmed by numerical findings. It encourages the confirmation that software and models will be employed.

We hope this will help lessen our nation's reliance on foreign resources. Using open-source software and tools, one may learn about the aviation industry and fluid dynamics while also

contributing our nation in the future by comparing theoretical calculations with actual experiments.

The air intake designed in this study was carried out with specified production constraints and limited computer power. In future studies, these limitations can be expanded, and optimization studies can be carried out with developing artificial intelligence algorithms.

In addition, experimental data can be obtained by subjecting the produced geometry to the wind tunnel test. The experimental data obtained here can be compared with the analysis studies.

7. REFERENCES

[1] Brandon, J. (2020) S-Duct Inlet Design for a Highly Maneuverable Unmanned Aircraft, Thesis, The Ohio State University, Ohio, USA

[2] NASA Glenn Research Center; (Inlets (nasa.gov))

[3] El-Sayed, A. & Emeara, M. (2016) INTAKE OF AERO-ENGINES: A CASE STUDY, Zagazig University, Aswan, Egypt

[4] Samet Aslan, D. Funda Kurtuluş, Ender Hepkaya, Sefa Yılmaztürk (2018) Numerical Imvestigation of a Serpentine Inlet Validated with Experimental Results for Different Turbulence Models, Turkey

[5] Wellborn, S.R., Reichert, B.A., Okiishi, T.H. (1992). An experimental investigation of the flow in a diffusing S-duct. 28th Joint Propulsion Conference and Exhibit. 6–8 July, Nashville, AIAA-92-3622.

[6] Aslan S., Yilmazturk S., Kurtulus D.F. (2015). Aerodynamic investigation of a serpentine inlet design for a micro-turbojet engine powered aircraft, International Symposium on Sustainable Aviation, Istanbul.

[7] Zhuoran Liu, Caizheng Wang, Ke Zhang, Zhuo Zhao, Zhifeng Xie (2021) Research on Computational Method of Supersonic Inlet/Isolator Internal Flow, China

[8] Anderson,W.E.;Wong, N.D. Experimental Investigation of a Large Scale, Two Dimensional, Mixed-Compression Inlet System-Performance at Design Conditions, M=3.0; NASA: NASA Ames Research Center Moffett Field, CA, USA, 1970.

[9] Reinartz, B.U.; Herrmann, C.D.; Ballmann, J.; Koschel, W.W. Aerodynamic performance analysis of a hypersonic inlet isolator using computation and experiment. J. Propuls. Power 2003, 19, 868–875.

[10] https://www.grc.nasa.gov/www/wind/valid/tutorial/spatconv.html

8. APPENDICES

MATLAB code for s-duct geometry:

```
clear all
clc
n=25;
Dc=0.144;              % Highlight(Entry) Diameter, Capture area (m)
Dsphere=20*Dc;         % Diameter of Sphere (m)
Dthroat=0.1288;        % Throat Diameter (m)
L=0.4572;              % Duct Length (m)
Daip=0.1524;           % Diameter at Engine Face (m)
H=1.065*Dthroat;       % Offset from centerline curvature (m)
x=linspace(0,L,n);     % Location at x(m)
z=-0.15.*L.*(1-cos(pi.*x./L));    % Location at z(m)
D=Dthroat+(Daip-Dthroat).*(3.*(1-(x./L)).^4-4.*(1-(x./L)).^3+1);% Diameter (m)
r=D./2;                % Radius (m)
r=[r]';
D=[D]';
x=[x]';
z=[z]';
y=linspace(0,0,n);
y=[y]';
T=table(x,y,z,D,r)
```

Table A. 1 S-duct geometry data

x(m)	y(m)	z(m)	D(m)	r(m)
0	0	0	0.1288	0.0644
0.01905	0	-0.00059	0.12903	0.064516
0.0381	0	-0.00234	0.12968	0.064839
0.05715	0	-0.00522	0.13066	0.065331
0.0762	0	-0.00919	0.13191	0.065957
0.09525	0	-0.01417	0.13337	0.066686
0.1143	0	-0.02009	0.13498	0.067488
0.13335	0	-0.02683	0.13667	0.068337
0.1524	0	-0.03429	0.13841	0.069207
0.17145	0	-0.04234	0.14016	0.070078
0.1905	0	-0.05083	0.14186	0.07093
0.20955	0	-0.05963	0.14349	0.071746
0.2286	0	-0.06858	0.14503	0.072513

0.24765	0	-0.07753	0.14644	0.073218
0.2667	0	-0.08633	0.14771	0.073853
0.28575	0	-0.09482	0.14882	0.074411
0.3048	0	-0.10287	0.14978	0.074889
0.32385	0	-0.11033	0.15057	0.075285
0.3429	0	-0.11707	0.1512	0.075601
0.36195	0	-0.12299	0.15168	0.07584
0.381	0	-0.12797	0.15202	0.076009
0.40005	0	-0.13194	0.15223	0.076116
0.4191	0	-0.13482	0.15235	0.076174
0.43815	0	-0.13657	0.15239	0.076197
0.4572	0	-0.13716	0.1524	0.0762

MATLAB code for mesh independency study:

```
clc
clear all
PR_coarse = 0.9754 ;
PR_normal = 0.9756 ;
PR_fine = 0.9760 ;
p = abs(log((PR_coarse-PR_normal)/(PR_normal-PR_fine))/log(1.33))
Fs=1.25;
GCI_12 = Fs*abs(( PR_fine-PR_normal)/PR_fine)/(2^p-1)*100
GCI_23 = Fs*abs(( PR_normal-PR_coarse)/PR_normal)/(2^p-1)*100
GCI_23/((2^p)*GCI_12) % asymptotic range of converge
PR_RE = PR_fine + (PR_fine-PR_normal)/(2^p-1)
x = [0.67, 1, 1.33];
y = [0.9754, 0.9756 ,0.976];
plot(x,y)
xlabel('Grid Spacing')
ylabel('Pressure Recovery')
grid on
```

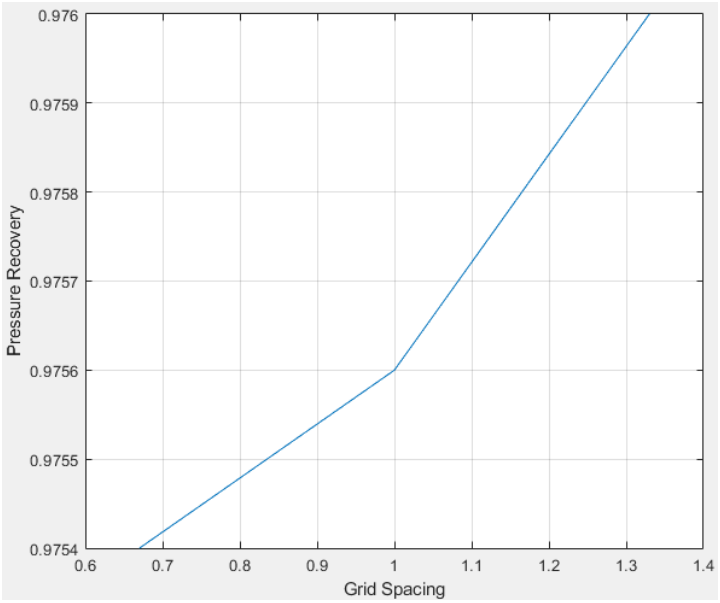

Figure A. 1 PR versus mesh intensity